Inorganic Chemistry

Article

Facile Synthesis and Characterization of Phosphorescent Pt(N^C^N)X Complexes

Zixing Wang,[†] Eric Turner,[†] Vanessa Mahoney,[†] Sijesh Madakuni,[†] Thomas Groy,[‡] and Jian Li*,[†]

[†]*School of Materials, Arizona State University, Tempe, Arizona 85287, United States, and*
[‡]*Department of Chemistry and Biochemistry, Arizona State University, Tempe, Arizona 85287, United States*

In order to investigate the ground state and excited state properties of Pt(N^C^N)X, we have prepared a series of Pt complexes, where N^C^N aromatic chelates are derivatives of *m*-di(2-pyridinyl)benzene (dpb) and X are monoanionic and monodentate ancillary ligands including halide and phenoxide. Facile synthesis of platinum *m*-di-(2-pyridinyl)benzene chloride and its derivatives, using controlled microwave heating, was reported. This method not only shortened the reaction time but also improved the reaction yield for most of the Pt complexes. Two Pt(N^C^N)X complexes have been structurally characterized by X-ray crystallography. The change of functional group does not affect the structure of the core Pt(N^C^N)Cl fragment. Both molecules pack as head-to-tail dimers, each molecule of the dimer related to the other by a center of inversion. The electrochemical studies of all Pt complexes demonstrate that the oxidation process occurs on the metal-phenyl fragment and the reduction process is associated with the electron accepting groups like pyridinyl groups and their derivatives. The maximum emission wavelength of the Pt(N^C^N)X complexes ranges between 471 and 610 nm, crossing the spectrum of visible light. Most of the Pt complexes are strongly luminescent ($\Phi = 0.32-0.63$) and have short luminescence lifetimes ($\tau = 4-7 \mu s$) at room temperature. The lowest excited state of the Pt(N^C^N)X complexes is identified as a dominant ligand-centered $^3\pi-\pi^*$ state with some ^{1}MLCT/^{3}MLCT character, which appears to have a larger ^{1}MLCT component than their bidentate and tridentate analogs. This results in a high radiative decay rate and high quantum yield for Pt(dpb)Cl and its analogs. However, the excited state properties of the Pt(N^C^N)X complexes are strongly dependent on the nature of the electron-accepting groups and substituents to the metal-phenyl fragment. A rational design will be needed to tune the emission energies of the Pt(N^C^N)X complexes over a wide range while maintaining their high luminescent efficiency.

Introduction

Square planar platinum (Pt) complexes have attracted a great deal of interest from academia and industry due to their potential application in many areas such as chemosensors,[1] photocatalysts,[2] organic light-emitting diodes (OLEDs),[3] and photovoltaic devices.[4] In recent years, an intensive research effort has been directed toward the development of Pt complexes as efficient phosphorescent emitters for displays[3,5] and lighting applications.[6,7] The strong spin−orbital coupling of the heavy metal ions like Ir(III) and Pt(II) ensures a high quantum yield of triplet emission for these cyclometalated metal complexes.[8−12] The phosphorescent OLEDs fabricated with this class of emitters can utilize all of the electro-generated

*Author to whom correspondence should be sent, e-mail: jian.li.1@asu.edu.

(1) (a) Kunugi, Y.; Mann, K. R.; Miller, L. L.; Exstrom, C. J. *J. Am. Chem. Soc.* **1998**, *120*, 589. (b) Peyratout, C. S.; Aldridge, T. K.; Crites, D. K.; McMillin, D. R. *Inorg. Chem.* **1995**, *34*, 4484.

(2) (a) Lu, W.; Mi, B. X.; Chan, M. C. W.; Hui, Z.; Che, C. M.; Zhu, N.; Lee, S. T. *J. Am. Chem. Soc.* **2004**, *126*, 4958. (b) Zhang, D.; Wu, L.-Z.; Zhou, L.; Han, X.; Yang, Q.-Z.; Zhang, L.-P.; Tung, C.-H. *J. Am. Chem. Soc.* **2004**, *126*, 3440.

(3) (a) Baldo, M. A.; O'Brien, D. F.; You, Y.; Shoustikov, A.; Sibley, S.; Thompson, M. E.; Forrest, S. R. *Nature* **1998**, *395*, 151. (b) Lin, Y. Y.; Chan, S. C.; Chan, M. C. W.; Hou, Y. J.; Zhu, N.; Che, C. M.; Liu, Y.; Wang, Y. *Chem.—Eur. J.* **2003**, *9*, 1263. (c) Cocchi, M.; Kalinowski, J.; Virgili, D.; Fattori, V.; Develay, S.; Williams, J. A. G. *Appl. Phys. Lett.* **2007**, *90*, 023506.

(4) (a) McGarrah, J. E.; Eisenberg, R. *Inorg. Chem.* **2003**, *42*, 4355. (b) Islam, A.; Sugihara, H.; Hara, K.; Singh, L. P.; Katoh, R.; Yanagida, M.; Takahashi, Y.; Murata, S.; Arakawa, H.; Fujihashi, G. *Inorg. Chem.* **2001**, *40*, 5371. (c) Shao, Y.; Yang, Y. *Adv. Mater.* **2005**, *17*, 2841. (d) Wong, W. -Y.; Wang, X.-Z.; He, Z.; Djurišić, A. B.; Yip, C.-T.; Cheung, K.-Y.; Wang, H.; Mak, C. S. K.; Chan, W.-K. *Nat. Mater.* **2007**, *6*, 521.

(5) (a) Cleave, V.; Yahioglu, G.; Barny, P. L.; Friend, R. H.; Tessler, N. *Adv. Mater.* **1999**, *11*, 285. (b) Gong, X.; Robinson, M. R.; Ostrowski, J. C.; Moses, D.; Bazan, G. C.; Heeger, A. J. *Adv. Mater.* **2002**, *14*, 581.

(6) (a) Adamovich, V.; Brooks, J.; Tamayo, A.; Alexander, A. M.; Djurovich, P. I.; D'Andrade, B. W.; Adachi, C.; Forrest, S. R.; Thompson, M. E. *New J. Chem.* **2002**, *26*, 1171. (b) Williams, E. L.; Haavisto, K.; Li, J.; Jabbour, G. E. *Adv. Mater.* **2007**, *19*, 197.

(7) (a) Yang, X.; Xing, Z.; Madakuni, S.; Li, J.; Jabbour, G. E. *Adv. Mater.* **2008**, *20*, 2405. (b) Yang, X.; Xing, Z.; Madakuni, S.; Li, J.; Jabbour, G. E. *Appl. Phys. Lett.* **2008**, *93*, 193305.

(8) Colombo, M. G.; Güdel, H. U. *Inorg. Chem.* **1993**, *32*, 3081.

(9) Strouse, G. F.; Güdel, H. U.; Bertolasi, V.; Ferretti, V. *Inorg. Chem.* **1995**, *34*, 5578.

(10) Lever, A. P. B. *Inorganic Electronic Spectroscopy*, 2nd ed.; Elsevier: New York, 1984; pp 174−178.

(11) (a) Wiedenhofer, H.; Schützenmeier, S.; von Zelewsky, A.; Yersin, H. *J. Phys. Chem.* **1995**, *99*, 13385. (b) Schmidt, J.; Wiedenhofer, H.; von Zelewsky, A.; Yersin, H. *J. Phys. Chem.* **1995**, *99*, 226.

(12) Yersin, H.; Donges, D. *Top. Curr. Chem.* **2001**, *214*, 81–186.

singlet and triplet excitons and achieve 100% photon/electron conversion efficiency.[13] Moreover, the square planar coordination geometry of Pt(II) complexes offers additional photochemical reactivity over six-coordinated octahedral Ir(III) complexes.[14] The mechanism of excimer formation due to the potential $\pi-\pi$ and metal—metal (Pt—Pt) interactions has been explored to fabricate a single-doped white OLED for lighting applications.[6,7] Thus, a better understanding of the ground state and excited state properties of Pt(II) complexes will allow us to tune their optical properties and explore the related applications more effectively.

It has been well documented that luminescence from cyclometalated Ir(III) and Pt(II) complexes originates from the admixture of ligand-centered (^{3}LC) states and metal-to-ligand-charge-transfer (MLCT) states through spin—orbit coupling.[8–12,15] Employing different cyclometalating ligands enables the excited state energy of Pt complexes to be varied over a wide spectral range, i.e., turning the emission color from red to blue.[16–19] However, the nature and energy level of excited states of Pt complexes could also be strongly affected by the change in the complex system. Compared with Pt(II) complexes with bipyridines and their analogues, which are typically nonemissive at room temperature,[14c,20] the cyclometalated Pt complexes are emissive in solution at room temperature with a less pronounced d—d quenching influence due to the existence of the cyclometalated carbon.[16,21] In addition to bidentate coordination like C^N [e.g., 2-phenylpyridine (ppy)] and C^C, Pt complexes with three classes of tridentate cyclometalating ligands have also been investigated, which include N^C^N aromatic chelate derivatives [e.g., *m*-di(2-pyridinyl)benzene (dpb)],[17,18] C^N^N aromatic chelate derivatives [e.g., 2-phenyl-bipyridine (phbpy)],[22,23] and C^N^C aromatic chelate derivatives [e.g., *m*-bis(phenyl)pyridine (bppy)].[24] The use of different classes of aromatic chelates will affect not only the photophysical properties of the single molecule but also the functionality of aggregates. For example, the complex consisting of a Pt ion, chloride, and *m*-di(2-pyridinyl)benzene, i.e., Pt(dpb)Cl, has been reported to have a high luminescent efficiency (around 0.6) and comparably short luminescent lifetime (around 10 μs),[17a] which makes Pt(dpb)Cl

and its derivatives highly desirable as emissive dopants for OLEDs.[17b] Efficient blue, green, and white OLEDs have been fabricated using classes of emitters like Pt(N^C^N)Cl.[7,17] However, the reason why Pt(dpb)Cl is more emissive than its bidentate analog platinum (2-phenylpyridinato-N,C$^{2'}$) acetylacetonate [(ppy)Pt(acac)] and tridentate analog platinum (2-phenyl-bipyridinyl) chloride [Pt(phbpy)Cl] is not well-understood. Williams and co-workers have studied the photophysical properties of Pt(dpb)Cl and its derivatives, where the 4 postion of the centered phenyl ring was modified with different aryl substituents.[18] The emission spectra of this class of Pt complexes can be shifted to a shorter or longer wavelength in a certain range with the use of electron-withdrawing or electron-donating aryl substituents, while the quantum yields and luminescent lifetimes are largely unaffected. Nonetheless, these structural modifications leave the core segment of Pt complexes intact by keeping the same electron-accepting group (i.e., pyridinyl groups) and the planar geometry of the molecules. Several interesting questions remain regarding excited state properties of Pt(N^C^N)Cl: to what extent can the excited state properties be controlled, and how do the changes of the ancillary ligands (i.e., replacing chloride) influence the excited state properties of Pt complexes?

In order to investigate the ground state and excited state properties of Pt(N^C^N)X, we have prepared a series of Pt complexes, where X are monoanionic and monodentate ancillary ligands including halide and phenoxide. The structures and abbreviations for the cyclometalated Pt complexes reported here are listed in Figure 1. Microwave-assisted heating was also explored to perform the Stille cross-coupling reactions as well as metal coordination reactions of Pt complexes. Thus, the one-week preparation of Pt complexes following literature reports[17,25] can be shortened to one day adopting this new synthetic method. The electrochemical and photophysical properties of the Pt(N^C^N)X complexes are discussed in detail. The electrochemical studies of all Pt complexes demonstrate that the highest occupied molecular orbital (HOMO) localizes on the metal-phenyl fragment, and the lowest unoccupied molecular orbital (LUMO) occupies dominantly on the electron accepting groups like pyridinyl groups and their derivatives. The lowest excited state of Pt(N^C^N)X complexes is identified as a dominant ligand-centered $^3\pi-\pi^*$ state with some ^{3}MLCT/^{1}MLCT character. The excited state properties of the Pt(N^C^N)X complexes can be strongly affected by changing the electron-accepting groups and molecular geometry.

Experimental Section

The microwave reactor (Discover, CEM Corp.) was used to perform the microwave flash heating reaction. The UV—visible spectra were recorded on a Cary 5G UV—vis—NIR spectrometer (Varian). Steady state emission experiments at room temperature were performed on a Horiba Jobin Yvon Fluoro-Log-3 spectrometer. Quantum efficiency measurements were carried out at room temperature in a solution of dichloromethane. Before the emission spectra were measured, the solutions were thoroughly bubbled by nitrogen inside of a glovebox with the content of oxygen less than 0.1 ppm. Solutions of coumarin 47 (coumarin 1; $\Phi = 0.73$, excited at 360 nm),[26] coumarin

(13) Adachi, C.; Baldo, M. A.; Thompson, M. E.; Forrest, S. R. *J. Appl. Phys.* **2001**, *90*, 5048.

(14) (a) Miskowski, V. M.; Houlding, V. H. *Inorg. Chem.* **1991**, *30*, 4446. (b) Houlding, V. H.; Miskowski, V. M. *Coord. Chem. Rev.* **1991**, *111*, 145. (c) Miskowski, V. M.; Houlding, V. H.; Che, C. M.; Wang, Y. *Inorg. Chem.* **1993**, *32*, 2518.

(15) Rausch, A. F.; Murphy, L.; Williams, J. A. G.; Yersin, H. *Inorg. Chem.* **2009**, *48*, 11407.

(16) Brooks, J.; Babayan, Y.; Lamansky, S.; Djurovich, P. I.; Tsyba, I.; Bau, R.; Thompson, M. E. *Inorg. Chem.* **2002**, *41*, 3055.

(17) (a) Williams, J. A. G.; Beeby, A.; Davies, E. S.; Weinstein, J. A.; Wilson, C. *Inorg. Chem.* **2003**, *42*, 8609. (b) Sotoyama, W.; Satoh, T.; Sawatari, N.; Inoue, H. *Appl. Phys. Lett.* **2005**, *86*, 153505.

(18) Farley, S. J.; Rochester, D. L.; Thompson, A. L.; Howard, J. A. K.; Williams, J. A. G. *Inorg. Chem.* **2005**, *44*, 9690.

(19) Che, C.-M.; Kwok, C.-C.; Lai, S.-W.; Rausch, A. F.; Finkenzeller, W. J.; Zhu, N.; Yersin, H. *Chem.—Eur. J.* **2010**, *16*, 233.

(20) Aldridge, T. K.; Stacy, E. M.; McMillin, D. R. *Inorg. Chem.* **1994**, *33*, 722.

(21) Balashev, K. P.; Puzyk, M. V.; Kotlyar, V. S.; Kulikova, M. V. *Coord. Chem. Rev.* **1997**, *159*, 109.

(22) Constable, E. C.; Henney, R. P. G.; Leese, T. A.; Tocher, D. A. *Chem. Commun.* **1990**, 513.

(23) (a) Lu, W.; Zhu, N.; Che, C.-M. *Chem. Commun.* **2002**, 900. (b) Che, C.-M.; Zhang, J.-L.; Lin, L.-R. *Chem. Commun.* **2002**, 2556. (c) Che, C.-M.; Fu, W.-F.; Lai, S.-W.; Hou, Y.-J.; Liu, Y.-L. *Chem. Commun.* **2003**, 118.

(24) Yam, V. W.-W.; Tang, R. P.-L.; Wong, K. M.-C.; Lu, X.-X.; Cheung, K.-K.; Zhu, N. *Chem.—Eur. J.* **2002**, *8*, 4066.

(25) Cárdenas, D. J.; Echavarren, A. M.; Ramírez de Arellano, M. C. *Organometallics* **1999**, *18*, 3337.

(26) Jones, G., II; Jackson, W. R.; Choi, C.-Y.; Bergmark, W. R. *J. Phys. Chem.* **1985**, *89*, 294.
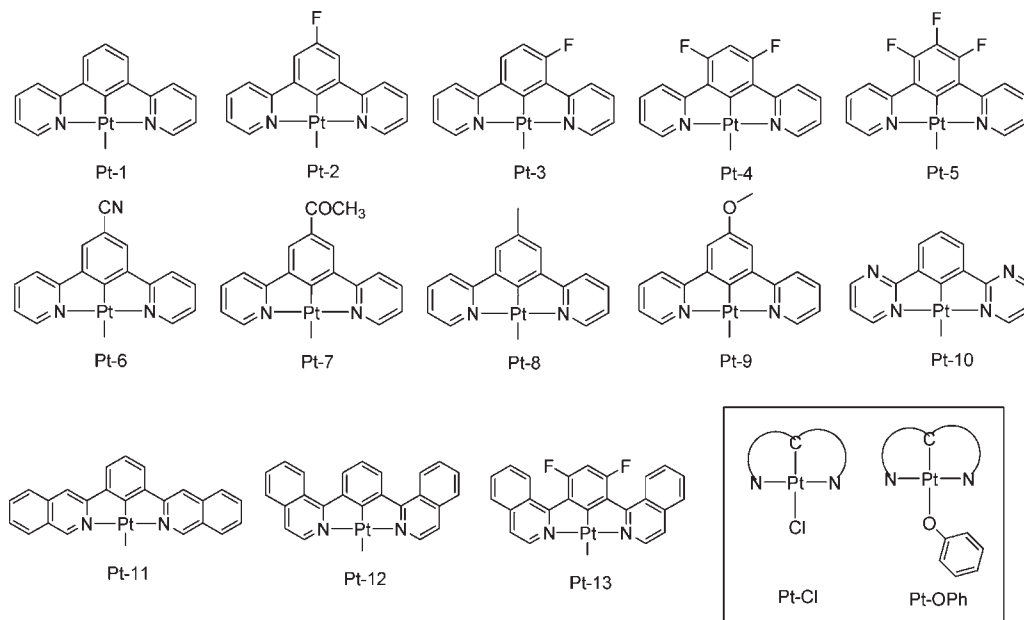
Figure 1. Structural formula and abbreviations used for the Pt(N^C^N)X complexes. The ancillary ligand X is chloride unless noted.

6 ($\Phi = 0.78$, excited at 420 nm),[27] and rhodamine B ($\Phi = 0.70$, excited at 510 nm)[28] in ethanol were used as references for Pt complexes with a selected emission range. The equation $\Phi_s = \Phi_r[(\eta_s^2 A_r I_s)/(\eta_r^2 A_s I_r)]$ was used to calculate the quantum yield, where Φ_s is the quantum yield of the sample, Φ_r is the quantum yield of the reference, η is the refractive index of the solvent, A_s and A_r are the absorbances of the sample and the reference at the wavelength of excitation, and I_s and I_r are the integrated areas of emission bands.[29] Phosphorescence lifetime measurements were performed on the same spectrometer with a time correlated single photon counting method using a LED excitation source. NMR spectra were recorded on a Varian Gemini-300, 400, or 500 MHz spectrometer with TMS as the internal reference, and chemical shifts were referenced to residual protiated solvent. Mass spectra were recorded on an Applied Biosystems Voyager-DE STR MALDI-TOF mass spectrometer. The Microanalysis Laboratory at Zhejiang University performed all elemental analysis on the Vario EL III Elemental Analyzer.

X-Ray Crystallography. X-ray diffraction data were collected on a Bruker SMART APEX CCD diffractometer with graphite-monochromated Mo Kα radiation ($\lambda = 0.71073$ Å) at 298(2) K for both Pt-4 and Pt-13. A sphere of diffraction data was collected up to a resolution of 0.84 Å for Pt-4 and 0.77 Å for Pt-13, and the intensity data were processed using the SAINT program. The cell parameters for the Pt complexes were obtained from the least-squares refinement of spots (from 1818 collected frames for each compound) using the SAINT program. Absorption corrections were applied by using SADABS.[30] All calculations for the structure determination were carried out using the SHELXTL package (version 6.14).[31] Initial Pt atomic positions were located by Patterson methods using XS, and the remaining structure of Pt-4 was found using difference maps and refined by least-squares methods using SHELXL-97 with 2451 independent reflections within the range of $\theta = 2.33-25.03°$ (completeness 100.0%). The Pt atomic positions for Pt-13 were determined by

Table 1. Crystal Data and Summary of Intensity Data Collection and Structure Refinement for Pt-4 and Pt-13

	Pt-4	Pt-13
empirical formula	$C_{16}H_9ClF_2N_2Pt$	$C_{24}H_{13}ClF_2N_2Pt$
fw	497.79	597.90
temp, K	298(2)	298(2)
wavelength, Å	0.71073	0.71073
cryst syst	monoclinic	triclinic
space group	$P2_1/n$	$P\bar{1}$
unit cell dimensions		
a (Å)	8.3088(12)	7.7675(12)
b (Å)	9.5462(14)	10.9813(17)
c (Å)	17.574(3)	11.7112(18)
α (deg)	90.00	83.038(3)
β (deg)	94.747(3)	71.048(2)
γ (deg)	90.00	75.310(2)
volume, Å^3	1389.2(4)	913.1(2)
Z	4	2
d_{calc}, Mg/m^3	2.380	2.175
abs coeff, mm^{-1}	10.311	7.864
F(000)	928	568
θ range for data collection, deg	2.430 to 25.096	2.602 to 27.563
reflns collected	10867	7174
indep reflns	2463	3204
refinement method	full-matrix least-squares on F^2	full-matrix least-squares on F^2
data/restraints/params	2451/0/199	3204/0/271
goodness-of-fit on F^2	1.120	1.131
final R indices [I > 2σ(I)]	0.0288	0.0397
R indices (all data)	0.0323	0.0435

Patterson synthesis using XS, and the remaining atoms were found in the difference maps. The structure was refined by least-squares methods using SHELXL-97 on 3204 reflections within the range of $\theta = 1.92-25.00°$ (completeness 99.9%). Calculated hydrogen positions were input and refined in a riding manner along with the attached carbons. A summary of the refinement details and resulting factors are given in Table 1.

Electrochemistry. Cyclic voltammetry and differential pulsed voltammetry were performed using a CH Instrument 610B electrochemical analyzer. Anhydrous DMF (Aldrich) was used as the solvent under a nitrogen atmosphere, and 0.1 M tetra(n-butyl)-ammonium hexafluorophosphate was used as the supporting

(27) Reynolds, G. A.; Drexhage, K. H. *Opt. Commun.* **1975**, *13*, 222–225.
(28) Arbeloa, F. L.; Ojeda, P. R.; Arbeloa, I. L. *J. Luminesc.* **1989**, *44*, 105.
(29) DePriest, J.; Zheng, G. Y.; Goswami, N.; Eichhorn, D. M.; Woods, C.; Rillema, D. P. *Inorg. Chem.* **2000**, *39*, 1955.
(30) Blessing, R. H. *Acta Crystallogr.* **1995**, *A51*, 33.
(31) Sheldrick, G. M. *SHELXTL*, version 6.14; Bruker Analytical X-ray System, Inc.: Madison, WI, 2003.

electrolyte. A silver wire was used as the *pseudo*-reference electrode. A Pt wire was used as the counter electrode, and glassy carbon was used as the working electrode. The redox potentials are based on the values measured from differential pulsed voltammetry and are reported relative to a ferrocenium/ferrocene (Fc^+/Fc) redox couple used as an internal reference (0.45 V vs SCE).[32] The reversibility of reduction or oxidation was determined using cyclic voltammetry.[33] As defined, if peak anodic and peak cathodic currents have an equal magnitude under the conditions of fast scan (100 mV/s or above) and slow scan (50 mV/s), then the process is *reversible*; if the magnitudes in peak anodic and peak cathodic currents are the same in fast scan but slightly different in slow scan, the process is defined as *quasi-reversible*; otherwise, the process is defined as *irreversible*.

Synthesis.   General Procedure for the Stille Coupling Following Literature Methods[25]. A mixture of substituted *m*-dibromobenzene (10 mmol), 2-(tri-*n*-butylstannyl)pyridine (11.4 g, 30 mmol), Pd(PPh$_3$)$_2$Cl$_2$ (70 mg, 0.1 mmol), and LiCl (2.55 g, 60 mmol) in toluene (70 mL) was stirred under reflux for 3 days under a nitrogen atmosphere. After cooling to room temperature, the reaction mixture was filtered. The filtrate was poured into water then extracted with dichloromethane. The combined organic phase was washed with brine and dried over MgSO$_4$. The solution was rotary-evaporated to dryness. The crude product mixture was then flash chromatographed on a silica column using a mixture of hexanes/ether (4:1) to give the product.

General Procedure for Microwave-Accelerated Stille Coupling Reaction. Under a nitrogen atmosphere, a mixture of substituted *m*-dibromobenzene (1 mmol), 2-(tri-*n*-butylstannyl)pyridine (1.0 mL, 3.0 mmol), Pd(PPh$_3$)$_2$Cl$_2$ (7 mg, 0.01 mmol), CuO (0.24 g, 3 mmol), and DMF (4 mL) was placed in a 10 mL Pyrex pressure vessel. The tube was capped and rapidly heated by the microwave reactor (2450 MHz, 200W). The reaction mixture was kept at 160 °C for 15 min by controlling the flow rate of cooling air. After cooling to room temperature, the reaction mixture was poured into 50 mL of ethyl acetate and was filtered. The filtrate was washed by water and dried over MgSO$_4$. The solution was rotary-evaporated to dryness. The crude product mixture was then flash chromatographed on a silica column using a mixture of hexane/ether (4:1) to give the product.

The ^{1}H NMR data of corresponding ligands (L^2–L^{10}) following the previous synthetic method are presented in the Supporting Information. The ligands of L^{11}–L^{13} adopt different synthetic procedures, which are also reported in the Supporting Information.

General Procedure for Metal Coordination Reaction Following Literature Methods[25]. A mixture of substituted *m*-di(2-pyridinyl)benzene (1 mmol), K$_2$PtCl$_4$ (0.41 g, 1 mmol), and acetic acid (60 mL) was stirred under reflux for 3 days in a nitrogen atmosphere. After cooling to room temperature, the reaction mixture was filtered. The precipitate was washed with methanol, water, ethanol, and ether. The crude product was further purified by recrystallization in DMSO/methanol or train sublimation.

General Procedure for Microwave-Accelerated Metal Coordination Reaction. Under a nitrogen atmosphere, a mixture of K$_2$PtCl$_4$, *m*-di(2-pyridinyl)benzene (1 mmol), and 3 mL of AcOH/H$_2$O (9:1, v/v) was placed in a 10 mL Pyrex pressure vessel. The tube was capped and rapidly heated by the microwave reactor (2450 MHz, 200 W). The reaction mixture was kept at 160 °C for 30 min by controlling the flow rate of cooling air. After cooling to room temperature, the reaction mixture was filtered. The precipitate was washed with methanol, water, ethanol, and ether. The crude product was further purified by recrystallization in DMSO/methanol or train sublimation. The reaction yields of Pt complexes through two different methods are presented in Table 3.

(32) Connelly, N. G.; Geiger, W. E. *Chem. Rev.* **1996**, *96*, 877.
(33) Harris, D. C. *Quantitative Chemical Analysis*, 6th ed.; W. H. Freeman and Company: New York; pp 394–396.

1.   Platinum [2,6-Di(2-pyridinyl-κN)-4-fluorophenyl-κC] Chloride [Pt-2]. ^{1}H NMR (500 MHz, CDCl$_3$): δ 7.25 (d, J = 10.0 Hz, 2H), 7.34 (ddd, J_1 = 1.5 Hz, J_2 = 5.5 Hz, J_3 = 8.0 Hz, 2H), 7.66 (dd, J_1 = J_2 = 8.0 Hz, 2H), 7.99 (ddd, J_1 = 1.5 Hz, J_2 = J_3 = 8.0 Hz, 2H), 9.39 (dd, J_1 = 5.5 Hz, J_2 = 21.0 Hz, 2H). HRMS (MALDI-TOF), *m/z* calcd for [C$_{16}$H$_{10}$ClFN$_2$Pt]: 479.0164. Found: 478.9798. Calcd for [M$^+$–Cl]: 444.0476. Found 444.0356. Anal. Calcd. for C$_{16}$H$_{10}$ClFN$_2$Pt: C, 40.05; H, 2.10; N, 5.84. Found: C, 39.16; H, 2.20; N, 5.89.

2.   Platinum [2,6-Di(2-pyridinyl-κN)-3-fluorophenyl-κC] Chloride [Pt-3]. ^{1}H NMR (500 MHz, CDCl$_3$): δ 6.84 (dd, J_1 = 8.5 Hz, J_2 = 11.5 Hz, 1H), 7.23 (ddd, J_1 = 1.0 Hz, J_2 = 5.5 Hz, J_3 = 7.5 Hz, 1H), 7.29 (ddd, J_1 = 2.0 Hz, J_2 = 5.5 Hz, J_3 = 7.0 Hz, 1H), 7.40 (dd, J_1 = 4.0 Hz, J_2 = 8.5 Hz, 1H), 7.58 (dd, J_1 = 5.5 Hz, J_2 = 8.0 Hz, 1H), 7.89–7.96 (m, 3H), 9.23 (dd, J_1 = 5.5 Hz, J_2 = 21.0 Hz, 1H), 9.33 (dd, J_1 = 5.5 Hz, J_2 = 21.0 Hz, 1H). HRMS (MALDI-TOF), *m/z* calcd for [C$_{16}$H$_{10}$ClFN$_2$Pt]: 479.0164. Found: 478.9971. Calcd for [M$^+$–Cl]: 444.0476. Found: 444.0448. Anal. Calcd. for C$_{16}$H$_{10}$ClFN$_2$Pt: C, 40.05; H, 2.10; N, 5.84. Found: C, 39.75; H, 2.25; N, 5.96.

3.   Platinum [3,5-Difluoro-2,6-di(2-pyridinyl-κN)-phenyl-κC] Chloride [Pt-4]. ^{1}H NMR (500 MHz, CDCl$_3$): δ 6.67 (t, J = 11.0 Hz, 1H), 7.30 (ddd, J_1 = 1.5 Hz, J_2 = 6.0 Hz, J_3 = 7.5 Hz, 2H), 7.89 (d, J = 7.5 Hz, 2H), 7.96 (ddd, J_1 = 1.5 Hz, J_2 = 7.5 Hz, J_3 = 7.5 Hz, 2H), 9.31 (dd, J_1 = 1.0 Hz, J_2 = 6.0 Hz, J_3 = 21.0 Hz, 2H). HRMS (MALDI-TOF), *m/z* calcd for [C$_{16}$H$_9$ClF$_2$N$_2$Pt]: 497.0070. Found: 496.9369. Calcd for [M$^+$–Cl]: 462.0382. Found: 462.0216. Anal. Calcd. for C$_{16}$H$_9$ClF$_2$N$_2$Pt: C, 38.61; H, 1.82; N, 5.63. Found: C, 38.10; H, 1.91; N, 5.74.

4.   Platinum [3,4,5-Trifluoro-2,6-di(2-pyridinyl-κN)-phenyl-κC] Chloride [Pt-5]. ^{1}H NMR (500 MHz, CDCl$_3$): δ 7.30 (ddd, J_1 = 1.5 Hz, J_2 = 5.5 Hz, J_3 = 7.5 Hz, 2H), 7.90 (d, J = 8.0 Hz, 2H), 7.96 (ddd, J_1 = 1.5 Hz, J_2 = 7.5 Hz, J_3 = 8.0 Hz, 2H), 9.32 (dd, J_1 = 5.5 Hz, J_2 = 21.5 Hz, 2H). HRMS (MALDI-TOF), *m/z* calcd for [C$_{16}$H$_8$ClF$_3$N$_2$Pt]: 514.9976. Found: 514.9945. Calcd for [M$^+$–Cl]: 480.0287. Found: 480.0506. Anal. Calcd. for C$_{16}$H$_8$ClF$_3$N$_2$Pt: C, 37.26; H, 2.66; N, 5.70. Found: C, 40.50; H, 3.10; N, 5.68.

5.   Platinum [2,6-Di(2-pyridinyl-κN)-4-cyano-phenyl-κC] Chloride [Pt-6]. ^{1}H NMR (500 MHz, CDCl$_3$): δ 7.45 (ddd, J_1 = 1.5 Hz, J_2 = 6.0 Hz, J_3 = 7.5 Hz, 2H), 7.73 (s, 2H), 7.79 (d, J = 8.0 Hz), 8.08 (ddd, J_1 = 1.5 Hz, J_2 = 7.5 Hz, J_3 = 8.0 Hz, 2H), 9.45 (dd, J_1 = 6.0 Hz, J_2 = 22.0 Hz, 2H). HRMS (MALDI-TOF), *m/z* calcd for [C$_{17}$H$_{10}$ClN$_3$Pt]: 486.0211. Found: 486.0336. Calcd for [M$^+$–Cl]: 451.0522. Found: 451.0664. Anal. Calcd. for C$_{17}$H$_{10}$ClN$_3$Pt: C, 41.94; H, 2.07; N, 8.63. Found: C, 39.80; H, 1.95; N, 8.40.

6.   Platinum   [2,6-Di(2-pyridinyl-κN)-4-acetylphenyl-κC] Chloride[Pt-7]. ^{1}H NMR (500 MHz, CDCl$_3$): δ 2.68 (s, 3H), 7.36 (ddd, J_1 = 1.5 Hz, J_2 = 5.5 Hz, J_3 = 7.5 Hz, 2H), 7.83 (d, J = 8.0 Hz, 2H), 8.03, (ddd, J_1 = 1.5 Hz, J_2 = 7.5 Hz, J_3 = 8.0 Hz, 2H), 8.07 (s, 2H), 9.40 (ddd, J_1 = 1.0 Hz, J_2 = 5.5 Hz, J_3 = 22.0 Hz, 2H). HRMS (MALDI-TOF), *m/z* calcd for [C$_{18}$H$_{13}$ClN$_2$OPt]: 503.0364. Found: 503.0198. Calcd for [M$^+$–Cl]: 468.0676. Found: 468.0892. Anal. Calcd. for C$_{18}$H$_{13}$ClN$_2$OPt: C, 42.91; H, 2.60; N, 5.56. Found: C, 42.06; H, 2.76; N, 5.60.

7.   Platinum [2,6-Di(2-pyridinyl-κN)-4-methylphenyl-κC] Chloride [Pt-8]. ^{1}H NMR (500 MHz, CDCl$_3$): δ 2.37 (s, 3H), 7.28 (dd, J_1 = 2.0 Hz, J_2 = 7.5 Hz, 2H), 7.29 (s, 2H), 7.66 (d, J = 8.0 Hz, 2H), 7.93 (ddd, J_1 = 2.0 Hz, J_2 = 7.5 Hz, J_3 = 8.0 Hz, 2H), 9.34 (ddd, J_1 = 1.0 Hz, J_2 = 6.0 Hz, J_3 = 22.0 Hz, 2H). HRMS (MALDI-TOF), *m/z* calcd for [C$_{17}$H$_{13}$ClN$_2$Pt]: 475.0415. Found: 475.0691. Calcd for [M$^+$–Cl]: 440.0726. Found: 440.1626. Anal. Calcd. for C$_{17}$H$_{13}$ClN$_2$Pt: C, 42.91; H, 2.75; N, 5.89. Found: C, 42.79; H, 2.71; N, 5.47.

8.   Platinum [2,6-Di(2-pyridinyl-κN)-4-methoxyphenyl-κC] Chloride [Pt-9]. ^{1}H NMR (500 MHz, CDCl$_3$): δ 3.90 (s, 3H), 7.10 (s, 2H), 7.28 (ddd, J_1 = 1.5 Hz, J_2 = 6.0 Hz, J_3 = 8.0 Hz, 2H), 7.65 (d, J = 8.0 Hz, 2H), 7.94 (ddd, J_1 = 1.5 Hz, J_2 = J_3 = 8.0 Hz, 2H), 9.34 (ddd, J_1 = 1.0 Hz, J_2 = 6.0 Hz, J_3 = 21.0 Hz, 2H).

HRMS (MALDI-TOF), m/z calcd for [C$_{17}$H$_{13}$ClN$_2$OPt]: 491.0364. Found: 491.0523. Calcd for [M$^+$−Cl]: 456.0676. Found: 456.0828. Anal. Calcd. for C$_{17}$H$_{13}$ClN$_2$OPt: C, 41.50; H, 2.66; N, 5.70. Found: C, 40.80; H, 2.79; N, 5.68.

9. Platinum [2,6-Di(2-pyrimidinyl-κN)-phenyl-κC] Chloride [Pt-10]. ^{1}H NMR (500 MHz, CDCl$_3$): δ 7.29 (dd, J_1 = 5.0 Hz, J_2 = 5.5 Hz, 2H), 7.36 (t, J = 8.0 Hz, 1H), 7.87 (d, J = 7.5 Hz, 2H), 8.94 (dd, J_1 = 5.0 Hz, J_2 = 2.5 Hz, 2H), 9.45 (ddd, J_1 = 2.5 Hz, J_2 = 5.0 Hz, J_3 = 20.5 Hz, 2H). Anal. Calcd. for C$_{14}$H$_9$ClN$_4$Pt: C, 36.26; H, 1.96; N, 12.08. Found: C, 36.16; H, 2.10; N, 12.47.

10. Platinum [2,6-di(3-isoquinolyl-κN)-phenyl-κC] chloride [Pt-11]. ^{1}H NMR (500 MHz, CDCl$_3$): δ 7.27 (t, J = 7.5 Hz, 1H), 7.49 (d, J = 7.5 Hz, 2H), 7.63 (ddd, J_1 = 8.0 Hz, J_2 = 7.0 Hz, J_3 = 1.5 Hz, 2H), 7.79 (ddd, J_1 = 8.0 Hz, J_2 = 7.0 Hz, J_3 = 1.5 Hz, 2H), 7.87 (d, J = 8.0 Hz, 2H), 7.97 (dd, J_1 = 4.0, J2 = 7.0 Hz, 2H), 8.07 (d, J = 8.0 Hz, 2H), 10.07 (dd, J = 23 Hz, 2H). Anal. Calcd. for C$_{24}$H$_{15}$ClN$_2$Pt: C, 51.31; H, 2.69; N, 4.99. Found: C, 50.73.97; H, 2.31; N, 5.27.

11. Platinum [2,6-Di(1-isoquinolyl-κN)-phenyl-κC] Chloride [Pt-12]. ^{1}H NMR (500 MHz, CDCl$_3$): δ 7.44 (t, J = 8.0 Hz, 1H), 7.68 (d, J = 6.5 Hz, 2H), 7.74 (ddd, J_1 = 1.5 Hz, J_2 = 8.5 Hz, J_3 = 8.0 Hz, 2H), 7.80 (ddd, J_1 = 1.5 Hz, J_2 = 8.5 Hz, J_3 = 6.5 Hz, 2H), 7.95 (d, J = 8.0 Hz, 2H), 8.29 (d, J = 8.0 Hz, 2H), 8.99 (d, J = 8.5 Hz, 2H), 9.52 (dd, J_1 = 6.5 Hz, J_2 = 18.5 Hz, 2H). Anal. Calcd. for C$_{24}$H$_{15}$ClN$_2$Pt: C, 51.31; H, 2.69; N, 4.99. Found: C, 50.23.97; H, 2.93; N, 5.04.

12. Platinum [3,5-Difluoro-2,6-di(1-isoquinolyl-κN)-phenyl-κC] Chloride [Pt-13]. ^{1}H NMR (500 MHz, CDCl$_3$): δ 6.91 (t, J = 12 Hz, 1H), 7.69−7.74 (m, 4H), 7.84 (ddd, J_1 = 1.0 Hz, J_2 = 8.0 Hz, J_3 = 8.0 Hz, 2H), 7.92 (d, J = 8.0 Hz, 2H), 8.51 (d, J = 8.5 Hz, 2H), 9.43 (dd, J_1 = 6.5 Hz, J_2 = 18.5 Hz, 2H). HRMS (MALDI-TOF), m/z calcd for [C$_{24}$H$_{13}$ClF$_2$N$_2$Pt]: 597.0383. Found: 597.0388. Calcd for [M$^+$−Cl]: 562.0695. Found: 562.0765. Anal. Calcd. for C$_{24}$H$_{13}$ClF$_2$N$_2$Pt: C, 48.21; H, 2.19; N, 4.69. Found: C, 47.97; H, 2.41; N, 4.82.

General Procedure for Complex Conversion from Pt−Cl to Pt-OPh. Under nitrogen, 1 mmol of the platinum complex was slowly added to a suspension of phenol (2 mml), KOH (1.5 mmol), and acetone (25 mL). After the mixture was stirred for 2 h, 50 mL of ether was added to the reaction mixture to generate more solids. The precipitate was filtrated off and washed by water, acetone, and ether. The yellow-to-red products with a yield of 40−60% were obtained from recrystallization in dichloromethane/acetone.

13. Platinum [3,5-Difluoro-2,6-di(2-pyridinyl-κN)-phenyl-κC] Phenoxide [Pt-4-OPh]. ^{1}H NMR (500 MHz, DMSO-d_6): δ 6.37 (td, J_1 = 7.0 Hz, J_2 = 1.0 Hz, 1H), 6.84−6.86 (m, 2H), 6.95−6.98 (m, 2H), 7.14 (t, J = 11.5 Hz, 1H), 7.53 (ddd, J_1 = 1.5 Hz, J_2 = 6.0 Hz, J_3 = 7.5 Hz, 2H), 7.96 (d, J = 7.5 Hz, 2H), 7.82 (ddd, J_1 = 1.5 Hz, J_2 = 7.5 Hz, J_3 = 7.5 Hz, 2H), 8.47 (ddd, J_1 = 1.0 Hz, J_2 = 6.0 Hz, J_3 = 15.0 Hz, 2H). Anal. Calcd. for C$_{22}$H$_{14}$F$_2$N$_2$OPt: C, 47.57; H, 2.54; N, 5.04. Found: C, 47.16; H, 2.60; N, 5.21.

14. Platinum [2,6-Di(1-isoquinolyl-κN)-phenyl-κC] Phenoxide [Pt-12-OPh]. ^{1}H NMR (500 MHz, CDCl$_3$): δ 6.58 (t, J = 7.0 Hz, 1H), 7.14−7.17 (m, 2H), 7.19−7.22 (m, 2H), 7.43 (t, J = 8.0 Hz, 1H), 7.61 (d, J = 6.5 Hz, 2H), 7.76 (ddd, J_1 = 1.5 Hz, J_2 = 8.5 Hz, J_3 = 8.0 Hz, 2H), 7.83 (ddd, J_1 = 1.5 Hz, J_2 = 8.5 Hz, J_3 = 6.5 Hz, 2H), 7,92 (d, J = 8.0 Hz, 2H), 8.31 (d, J = 8.0 Hz, 2H), 8.82 (dd, J_1 = 6.5 Hz, J_2 = 18.5 Hz, 2H), 9.52 (d, J = 8.5 Hz, 2H). Anal. Calcd. for C$_{30}$H$_{20}$N$_2$OPt: C, 58.16; H, 3.25; N, 4.52. Found: C, 57.71; H, 3.71; N, 4.68.

15. Platinum [3,5-Difluoro-2,6-di(1-isoquinolyl-κN)-phenyl-κC] Phenoxide [Pt-13-OPh]. ^{1}H NMR (500 MHz, CDCl$_3$): δ 7.08−7.13 (m, 4H), 7.28−7.32 (m, 2H), 7.65 (ddd, J_1 = 1.5 Hz, J_2 = 7.0 Hz, J_3 = 8.0 Hz, 2H), 7.87 (ddd, J_1 = 1.5 Hz, J_2 = 7.0 Hz, J_3 = 8.0 Hz, 2H), 7.99 (d, J = 8.0 Hz, 2H), 8.05 (d, J = 8.5 Hz,

Scheme 1. Synthesis of *m*-Di(2-pyridinyl)benzene and Pt(N^C^N)Cl Complexes
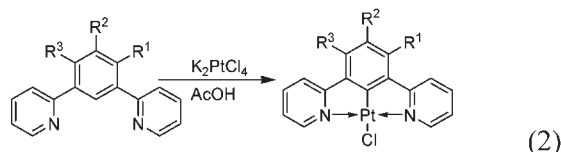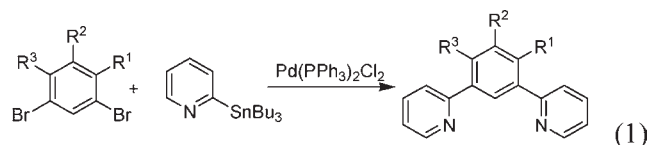
2H), 8.68 (d, J = 8.5 Hz, 2H), 9.16 (d, J_1 = 6.5 Hz, 2H). Anal. Calcd. for C$_{30}$H$_{18}$F$_2$N$_2$OPt: C, 54.96; H, 2.77; N, 4.27. Found: C, 55.7; H, 3.25; N, 3.81.

Results and Discussion

Synthesis and Characterization. Cárdenas et al. reported a two-step synthesis for Pt(N^C^N)Cl,[25] using the Stille cross-coupling reaction[34] followed by a coordination reaction. However, each step required at least 3 days to complete. Thus, a week of preparation was needed to synthesize a new Pt complex. In high-throughput chemistry, it is important to decrease the reaction time as well as to effectuate the purification procedure. It is well documented that microwave flash heating can dramatically reduce reaction time (from days and hours to minutes and seconds). Specifically, facile syntheses of cyclometalated metal complexes including [Ru(bpy)$_3$]$^{2+}$, [Ir(bpy)$_3$]$^{3+}$, and Ir(ppy)$_3$ have previously been explored.[35−37] Thus, it is worthy to explore if the microwave irradiation method can expedite the process of the Stille cross-coupling reaction[38] and the metal coordination reaction (Scheme 1).

The palladium-catalyzed Stille cross-coupling reactions of 1,3-dibromobenzene derivatives with 2-(tri-*n*-butylstannyl)pyridine were previously carried out in the presence of lithium chloride (LiCl) in refluxed toluene for 3 days with a 75% yield.[25] The initial set of microwave experiments was carried out using 1,3-dibromobenzene, 2-(tri-*n*-butylstannyl)pyridine (3 equiv), LiCl (6 equiv), and a catalytic amount of bis(triphenylphosphine)palladium(II) chloride (5% equiv). The reactions were performed under an atmosphere of nitrogen in sealed Pyrex vessels. This preliminary survey was carried out in toluene, a 9:1 (v/v) mixture of toluene/N,N-dimethylformamide (DMF), and pure DMF to evaluate and optimize the solvent conditions used in the microwave heating. However, the expected product was barely detectable under any of these conditions. When copper oxide

(34) (a) Stille, J. K. *Angew. Chem., Int. Ed. Engl.* **1986**, *25*, 508. (b) Michell, T. N. *Synthesis* **1992**, 803. (c) Ritter, K. *Synthesis* **1993**, 735. (d) Farina, V.; Roth, G. P. In *Advances in Metal-Organic Chemistry*; Liebeskind, L. S., Ed.; JAI Press Inc: Greenwich, CT, 1996; Vol. 5, p 1.
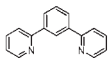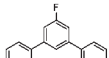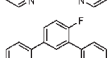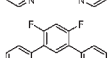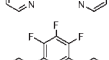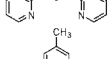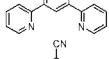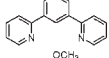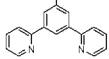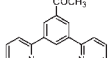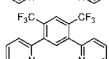
(35) Tastumura-Noue, T.; Tanabe, M.; Minami, T.; Ohashi, T. *Chem. Lett.* **1994**, *23*, 2443.

(36) Yoshikawa, N.; Musuda, Y.; Tastumura-Noue, T. *Chem. Lett.* **2000**, *29*, 1206.

(37) (a) Saito, K.; Matsusue, N.; Kanno, H.; Hamada, Y.; Takahashi, H.; Matsumura, T. *Jpn. J. App. Phys.* **2004**, *43*, 2733. (b) Konno, H.; Sasaki, Y. *Chem. Lett.* **2003**, *32*, 252.

(38) Larhed, M.; Hoshino, M.; Hadida, S.; Curran, D. P.; Hallberg, A. *J. Org. Chem.* **1997**, *62*, 5583.

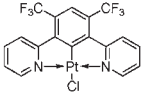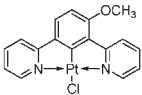**Table 2.** The Stille Cross-Coupling Reaction Yields under Two Conditions[a]

entry	product	yield-A (%)	yield-B (%)
1		67	65
2		70	65
3		65	60
4		74	75
5		66	66
6		72	79
7		81	76
8		69	60
9		71	70
10		72	70
11		72	73

[a] Method A: Substituted *m*-dibromobenzene (1 mmol), 2-(tri-*n*-butylstannyl)pyridine (3.0 equiv), CuO (3.0 equiv), Pd(PPh₃)₂Cl₂ (2% equiv), DMF, 150 °C (sealed tube), microwave heating for 15 minutes. Method B: Substituted *m*-dibromobenzene (1 mmol), 2-(tri-*n*-butylstannyl)pyridine (3.0 equiv), LiCl (6.0 equiv), Pd(PPh₃)₂Cl₂ (2% equiv), toluene, reflux for 3 days.

(CuO) replaced LiCl as the base, the reaction yield improved only if pure DMF was used as the solvent.[39] The failure of other solvent combinations can be partially attributed to the low microwave absorption of toluene.[40] To study the full scope of the procedure, a series of *m*-di(2-pyridinyl)benzene derivatives was prepared under both conditions (methods A and B in Table 2). All reactions provided fair to good yields of the isolated products after a workup procedure including filtration, extraction, and subsequent flash column chromatography. The change of substituents (from the electron donating group to the electron withdrawing group) did not influence the reaction outcome.

A rich chemistry of Pt ions with the cyclometalating tridentate ligands has been approached, including platinum complexes of N^N^C-binding ligands,[23c,41] C^N^C-binding ligands,[24] and a N^C^N-coordinating tridentate ligand.[17,18] Generally, the metal coordination of these complexes will take several days. For example, Pt(dpb)Cl can be obtained in a good yield after a 3-day reaction between dpb and potassium tetrachloroplatinate (K₂PtCl₄) in a refluxed solution of

Table 3. The Metal Coordination Reaction Yields under Two Conditions[a]

entry	Product	yield-A (%)	yield-B (%)
1	Pt-1	80%	70%
2	Pt-2	84%	75%
3	Pt-3	64%	60%
4	Pt-4	84%	80%
5	Pt-5	86%	90%
6	Pt-6	90%	62%
7	Pt-7	72%	66%
8	Pt-8	42%	31%
9	Pt-9	21%	20%
10		53%	37%
11		<5%	<5%
12	Pt-13	84%	85%

[a] Method A: Substituted *m*-di(2-pyridinyl)benzene (1 mmol), K₂PtCl₄ (0.42 g, 1 mmol), AcOH/H₂O (9:1, v/v), 160 °C (sealed tube), microwave heating for 30 minutes. Method B: Substituted *m*-di(2-pyridinyl)benzene (1 mmol), K₂PtCl₄ (0.42 g, 1 mmol), AcOH, reflux for 3 days.

acetic acid.[17a] Here, microwave-assisted synthesis of platinum complexes was performed as follows: a suspension of K₂PtCl₄ (1 mmol), dpb (1 mmol), and 3 mL of AcOH/H₂O (9:1, v/v) was sealed in a 10 mL Pyrex vessel. The vessel was set up in the microwave reactor and irradiated at different temperatures and power settings and for various durations. After cooling to room temperature, the product precipitated from the solution and was further purified through recrystallization in dimethyl sulfoxide/methanol or train sublimation. Our experimental results showed that a high reaction yield (80%) can be realized in a 30 min reaction at 160 °C using 200 W. This reaction yield is much higher than the literature reported synthesis of cyclometalated Ir complexes using microwave heating.[37]

The reactions of substituted dpb were studied next to determine the effect of the substituents (Table 3). When an electron-donating group was introduced on the phenyl ring, the yield of complexes decreased significantly (entries 6, 8, and 11). Conversely, the yield increased when an electron-withdrawing group, such as fluorine and a cyano group, was introduced (entries 2, 4, 5, 7, and 12). A similar trend was also observed under the conditions of normal oil heating. A hindering group such as isoquinolin-1-yl did not affect the

(39) Gibbs, R. A.; Krishnan, U.; Dolence, J. M.; Poulter, C. D. *J. Org. Chem.* **1995**, *60*, 7821.
(40) Kappe, C. O. *Angew. Chem., Int. Ed.* **2004**, *43*, 6250.
(41) Lai, S.-W.; Chan, M. C. W.; Cheung, T.-C.; Peng, S.-M.; Che, C.-M. *Inorg. Chem.* **1999**, *38*, 4046.

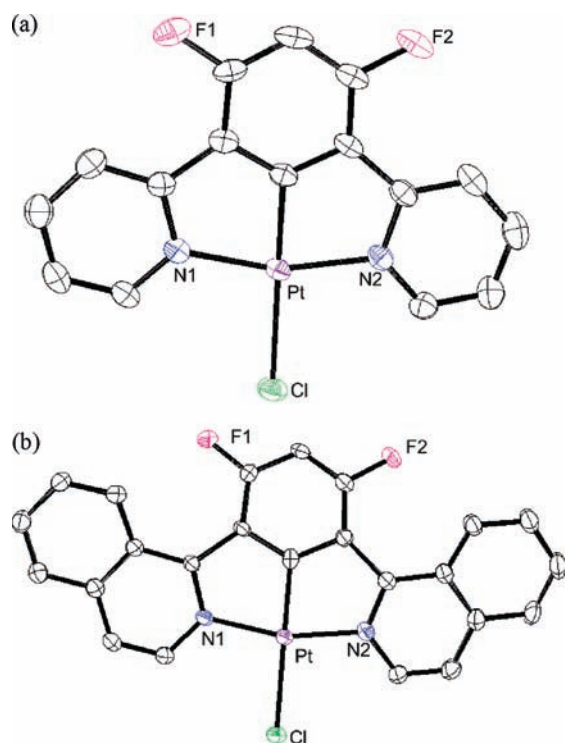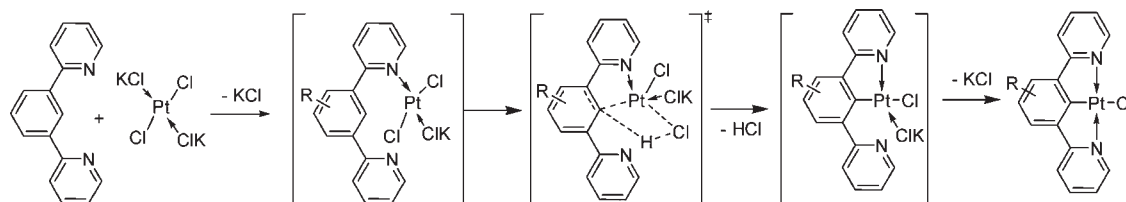**Scheme 2.** Proposed Mechanism for the Metal Coordination Reaction

Figure 2. ORTEP drawings of (a) Pt-4 and (b) Pt-13. The thermal ellipsoids for the image represent a 25% probability limit. The hydrogen atoms are omitted for clarity.
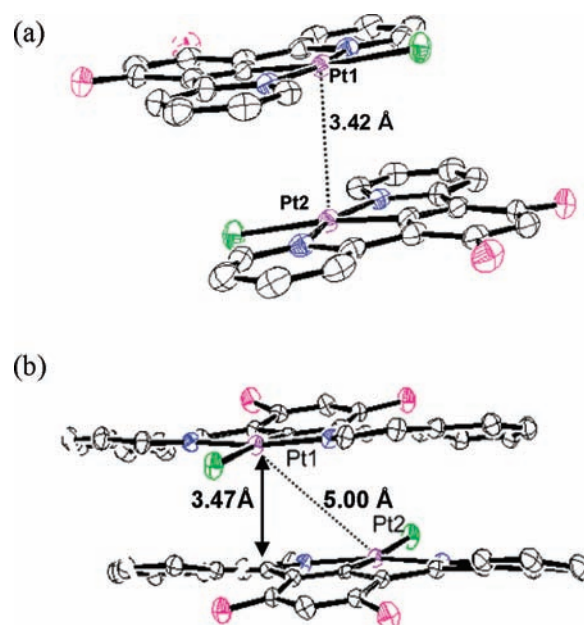

Figure 3. ORTEP drawings of (a) Pt-4, and (b) Pt-13 in a dimeric form. The thermal ellipsoids for the image represent a 25% probability limit. The hydrogen atoms are omitted for clarity. The dotted line indicates the shortest distance between two Pt atoms, and the solid line with double arrows indicates the shortest distance between the Pt atom and the least-squares plane of Pt−N−C−N.

reaction yield. A high coordination reaction yield was observed under both conditions (entry 12).

A possible reaction mechanism has been proposed in order to uncover the influence of substituents on the yield of metal coordination reactions. Typically, a ligand coordinates to a metal center, and a proximal C−H bond is activated, forming a chelate ring.[42] The coordination reaction can be formally considered as a multicentered pathway involving a nucleophile-assisted electrophilic reaction (Scheme 2).[42,43] Here, the nucleophile is a chloride ion. The substituents can affect the coordination reactions by influencing the C−H bond activation. When the electron-withdrawing group was introduced onto the phenyl ring, the electron density at the C−H bond was decreased. This increased the C−H bond acidity, resulting in more active bond cleavage.

Single crystals of Pt-4 and Pt-13 were prepared by slow sublimation. Molecular plots of Pt-4 and Pt-13 are shown in Figures 2 and 3. The crystallographic data are also given in Table 1. The selected bond lengths, plane-to-plane distances, and Pt−Pt distances for Pt-1,[25] Pt-4, and Pt-13 are

Table 4. Selected Bond Distances and Plane-to-Plane Distance (Å) for Pt Complexes Discussed in the Paper

	Pt−C	Pt−N$_1$	Pt−N$_2$	Pt−Cl	Pt···Pt	Pt···plane
Pt-1[25]	1.907(8)	2.033(6)	2.041(6)	2.417(2)	4.85	3.40
Pt-4	1.910(6)	2.028(5)	2.043(5)	2.4124(15)	3.42	3.38
Pt-13	1.918(8)	2.009(7)	2.021(7)	2.412(2)	5.00	3.47

provided in Table 4. Both Pt-4 and Pt-13 molecules have a distorted square planar geometry. Moreover, the change of functional group does not affect the structure of the core Pt(N^C^N)Cl fragment. The bond lengths of Pt−C, Pt−N$_1$, Pt−N$_2$, and Pt−Cl are similar for all of these three complexes. Similar to the literature reported Pt-1 molecules,[25] both Pt-4 and Pt-13 molecules pack as head-to-tail dimers, each molecule of the dimer related to the other by a center of inversion (Figure 3). The dimers have a plane-to-plane separation of 3.38 Å for Pt-4 and 3.47 Å for Pt-13, indicative of moderate π−π interactions (Figure 3). However, Pt-4 and Pt-13 have different levels of metal−metal interaction due to different molecular geometries. The shortest Pt−Pt distance (3.42 Å) of Pt-4 is much smaller than those of Pt-1 (4.85 Å)[25] and Pt-13 (5.00 Å). The difference can be attributed to the unflattened structure of Pt-13 created by changing pyridinyl groups to isoquinonyl groups.

(42) Ryabov, A. D. *Chem. Rev.* **1990**, *90*, 403.
(43) Jawad, J. K.; Puddephatt, R. J.; Stalteri, M. A. *Inorg. Chem.* **1982**, *21*, 332.

Table 5. Redox Properties of Pt(N^C^N)X Complexes[a]

Pt(N^C^N)X	$E_{1/2}^{Ox}$ (V)	$E_{1/2}^{Red}$ (V)	$\Delta E_{1/2}$ (V)
Pt-1	0.41	−2.18	2.59
Pt-2	0.47	−2.08	2.55
Pt-3	0.44	−2.09	2.53
Pt-4	0.50	−2.07	2.60
Pt-5	0.51	−2.07	2.58
Pt-6	0.59	−1.99	2.58
Pt-7	0.44	−2.07	2.53
Pt-8	0.40	−2.18	2.58
Pt-9	0.41	−2.16	2.57
Pt-10	0.5	−1.92	2.42
Pt-11	0.31	−2.08	2.39
Pt-12	0.34	−1.84	2.18
Pt-13	0.56	−1.74	2.28
Pt-4-OPh	0.36	−2.09	2.45
Pt-12-OPh	0.50	−1.83	2.33
Pt-13-OPh	0.58	−1.82	2.40

[a] Redox measurements were carried out in DMF solution. For all of the Pt complexes reported here, the oxidation process is irreversible and the first reduction process is reversible or quasi-reversible. The redox values are reported relative to Fc[+]/Fc.

Electrochemistry. The electrochemical properties of Pt(N^C^N)X complexes (1−13) were examined using cyclic voltammetry, and the values of redox potentials were determined using differential pulsed voltammetry (Table 5). All of the electrochemical data reported here were measured relative to an internal ferrocenium/ferrocene reference (Fc[+]/Fc). For all of the Pt complexes, they have one irreversible oxidation potential between 0.3 and 0.6 V and their first reduction potential between −1.8 and −2.2 V. The redox values of Pt-1 are slightly different than the literature values ($E_{1/2}^{Ox}$ = 0.43 V and $E_{1/2}^{red}$ = −2.03 V) due to the different choice of solvent systems.[18] The redox properties of Pt complexes are strongly affected by the structural modification of *m*-di(2-pyridinyl)benzene ligands. Incorporating the electron-withdrawing functional groups (like fluorine, cyano, and acetyl group) on the phenyl rings gives an increase in the oxidation potential and a decrease in the reduction potential, while introducing the electron-donating groups (like methyl and methoxyl groups) on the same location will lead to an increase in the reduction potential.[18,44] As the conjugated π systems of electron accepting groups increase, the complexes including Pt-11, Pt-12, and Pt-13 demonstrate a marked decrease in the reduction potential.

The electrochemical data support the fact that reduction occurs mainly on the ligands (i.e., pyridinyl group and its analogs) and oxidation is localized on the metal center, which is consistent with most literature reports on cyclometalated Pt complexes.[16] Due to the potential effects of the solvent on the square planar Pt(III) ions, the oxidation process of Pt(II) complexes is typically irreversible.[45] Compared with Pt(C^N)(acac) with similar cyclometalated ligands, the Pt(N^C^N)Cl complexes showed a marked decrease in their reduction potential. For example, the reduction value of Pt(dpb)Cl is more than 0.2 V lower than (ppy)Pt(acac) (−2.41 V vs Fc/Fc[+]).[16] This can be possibly attributed to the extended conjugation of tridentate N^C^N ligands compared with the bidentate C^N ligands. For selected Pt(N^C^N)X complexes, the change of ancillary ligands from chloride to phenoxide appeared to have a small influence on the electrochemical properties of Pt complexes. The oxidation and reduction values of Pt complex phenoxides are comparable to their chloride analogs.

Electronic Spectroscopy. The room temperature (RT) absorption and emission spectra and low-temperature (77 K) emission spectra were recorded for all Pt(N^C^N)X complexes (Table 6). A comparison of absorption features among Pt-1, Pt-4, Pt-9, and Pt-12 is shown in Figure 4. All of the Pt complexes exhibit very strong absorption bands below 300 nm ($\varepsilon > 1 \times 10^4$ L mol^{-1}cm^{-1}) due to $^1\pi-\pi^*$ transitions localized on N^C^N ligands (LC), together with a set of intense bands in the region 320−460 nm ($\varepsilon > 2 \times 10^3$ L mol^{-1}cm^{-1}), which are attributed to MLCT transitions involving both the cyclometalating ligands and platinum metal ions. Much weaker energy absorption bands between 440 and 600 nm ($\varepsilon < 200$ L mol^{-1} cm^{-1}) are identified as a triplet transition (T_1) on the basis of the small energy shift between absorption and emission at room temperature. The structural changes of Pt complexes have a strong influence on the absorption bands associated with ^{1}MLCT and T_1 transitions. Compared with Pt-1, adding electron-withdrawing groups to the phenyl ring (e.g., Pt-4) leads to an increase in ^{1}MLCT and T_1 transition energies. On the other hand, adding electron-donating groups to the phenyl ring (e.g., Pt-9) or replacing with lower energy electron-accepting groups (e.g., Pt-12) will decrease the energies of ^{1}MLCT and T_1 transitions. However, while ^{1}MLCT transition energies (for Pt-9 and Pt-12) decrease with minor changes in intensity, the decrease in the T_1 absorption energies coincides with a clear decrease in the extinction coefficient (Figure 4, inset).

The room temperature and 77 K emission spectra of Pt-1, Pt-4, Pt-9, and Pt-12 are shown in Figure 5. The emission spectra of these Pt complexes are affected strongly due to the structural changes. In general, the introduction of the electron-withdrawing groups on the phenyl ring, associated with an increase of oxidation potential, shifts the emission spectra to shorter wavelengths. On the other hand, adding the electron-donating groups on the phenyl rings will not only decrease the oxidation potential but also lower the emission energies of Pt complexes. Similarly, the red-shifted emission spectrum of Pt-12 due to the replacement of isoquinonyl groups concurred with a drop in the reduction potential. Such substitution effects have been observed for previously reported tricyclometalated iridium complexes and bidentate platinum complexes.[16]

Most of the Pt(N^C^N)Cl complexes, i.e., keeping the core segment of Pt-1, are strongly luminescent (Φ = 0.32−0.63) and have short luminescence lifetimes (τ = 4−7 μs) at room temperature, similar to values reported for Pt-1.[17,25] Exceptions are complexes with isoquinolyl or quinolyl groups. For example, the Φ values of Pt-12 and Pt-13 are less than 0.10, and the τ of Pt-11 is more than 40 μs. The radiative (k_r) and nonradiative decay (k_{nr}) rates can be calculated from the room temperature Φ and τ data.[46] The k_r values of the

(44) Kulikova, M.; Balashev, K. P.; Kvam, P. I.; Songstad, J. *Russ. J. Gen. Chem.* **2000**, *70*, 163.

(45) Kvam, P.-I.; Puzyk, M. V.; Balashev, K. P.; Songstad, J. *Acta Chem. Scand.* **1995**, *49*, 335–343.

(46) The equations $k_r = \Phi/\tau$ and $k_{nr} = (1 - \Phi)/\tau$ were used to calculate the rates of radiative and nonradiative decay, where Φ is the quantum efficiency and τ is the luminescence lifetime of the sample at room temperature.

Table 6. Photophysical Properties of Pt(N^C^N)X Complexes[a]

Pt(N^C^N)X	abs, λ(nm) {ε, $10^3 cm^2 mol^{-1}$}	emission at RT λ_{max}(nm)	τ(μs)	Φ_{PL}	k_r, $10^5 s^{-1}$	k_{nr}, $10^5 s^{-1}$	emission at 77 K λ_{max}(nm)	τ(μs)
Pt-1	255(25.2), 289(21.1), 319(6.1), 379(8.6), 402(7.0), 452(0.15), 485(0.14)	490	7.2	0.60	0.83	0.55	486	5.8
Pt-2	257(33.0), 278(26.3), 290(28.2), 377(8.8), 421(9.9), 496(0.12)	504	7.0	0.39	0.56	0.87	498	7.1
Pt-3	256(31.3), 286(23.3), 322(7.7), 335 (8.6), 380(10.4), 477(0.13)	481	6.5	0.52	0.80	0.74	477	5.6
Pt-4	261(30.9), 287(21.8), 322(8.2), 335(11.1), 375(10.4), 439(0.15), 468(0.14)	471	5.8	0.60	1.0	0.68	467	5.6
Pt-5	260(27.0), 289(19.9), 320(6.1), 334(6.8), 380(8.3), 405(4.6), 480(0.08)	490(sh), 517	7.8	0.46	0.59	0.69	481	5.7
Pt-6	268(43.2), 322(4.9), 380(8.1), 403(6.7), 478(0.13)	481	4.8	0.58	1.2	0.88	477	5.5
Pt-7	279(60.1), 330(9.7), 382(12.6), 398(10.5), 482(0.09)	485	6.5	0.63	0.97	0.57	482	6.1
Pt-8	260(25.0), 282(19.9), 293(21.9), 334(5.7), 382(6.8), 413(6.9), 496(0.09)	503	7.0	0.46	0.66	0.77	498	7.1
Pt-9	282(25.0), 293(27.6), 363(4.3), 379(6.3), 440(8.6), 510(0.08)	547	13	0.30	0.23	0.54	534	12.0
Pt-10	267(41.8), 382(10.6), 408(8.6), 479(0.17)	484	5.7	0.32	0.56	1.2	479	5.4
Pt-11	278(90.1), 362(28.8), 410(17.0), 490(0.03)	520 (sh), 558	40	0.20[a]	0.05	0.2	514	109
Pt-12	285(19.4), 334(5.7), 364(5.0), 422 (5.1), 445(4.5), 580(0.06)	592	3.5	0.072[b]	0.21	2.7	586	5.9
Pt-13	284(66.6), 329(15.2), 354(14.4), 369 (15.1), 407(18.5), 565(0.04)	594	4.4	0.10[b]	0.23	2.0	582	8.9
Pt-4-OPh	289(14.9), 335(6.1), 372(5.5), 468(0.25)	471	3.0	0.34	1.1	2.2	467	6.0
Pt-12-OPh	288(43.8), 334(6.3), 421(5.5), 445(4.3), 580(0.18)	592	3.4	0.035[b]	0.10	2.8	588	5.7
Pt-13-OPh	289(23.1), 375(20.0), 413(13.2), 575(0.03)	610	4.3	0.05[b]	0.11	2.2	594	10.6

[a] The room temperature absorption and emission spectra were measured in a solution of dichloromethane. The emission spectra at 77 K were measured in a solution of 2-methyl-THF. Coumarin 47 was used as a reference for quantum efficiency measurement unless noted: (a) Coumarin 6, (b) Rhodamine B.
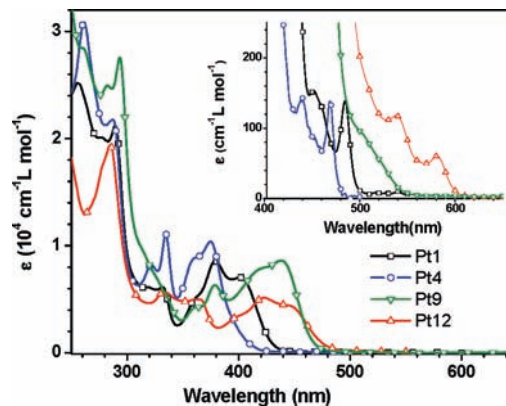

Figure 4. The comparison of absorption spectra of Pt-1, Pt-4, Pt-9, and Pt-12 in CH_2Cl_2 at room temperature. The T_1 absorption transitions are shown in the inset.
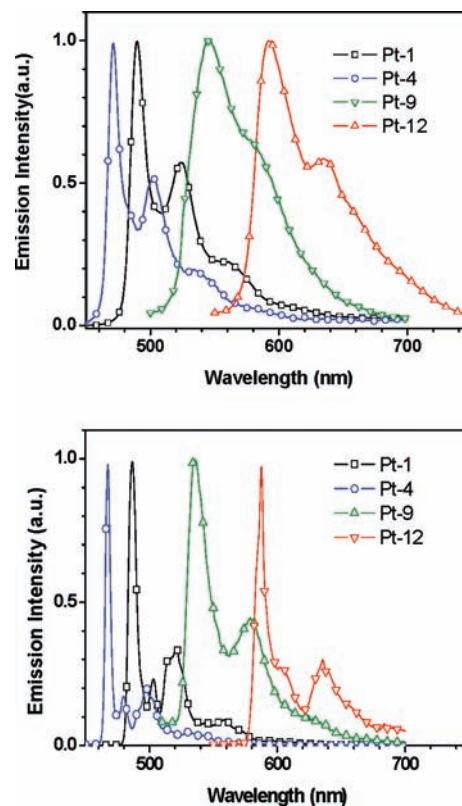

Figure 5. Room temperature (top) and 77 K emission (bottom) spectra of Pt-1, Pt-4, Pt-9, and Pt-12. 2-MeTHF was used for low temperature measurement instead of CH_2Cl_2.

Pt(N^C^N)Cl complexes range between 1.2×10^5 and 5×10^3 s^{-1}, which are strongly structure-dependent. The derivatives of Pt-1 maintain very high k_r values, although it appears to decrease 1−2 fold by adding an electron-donating group to the phenyl rings. Moreover, the k_r values are around 1 order of magnitude lower, while the pyridinyl groups are replaced by isoquinolyl or quinolyl groups (e.g., Pt-11 and Pt-12). The k_{nr} values span a narrower range of values (2.9×10^5 to 2×10^4 s^{-1}) and tend to increase as the emission energy decreases, indicating an observation of energy gap law.[47,48] All of the Pt(N^C^N)Cl complexes are intensely emissive at low temperatures (77 K), and most have short luminescence lifetimes ($\tau = 5-12\,\mu$s), except Pt-11 has a luminescent lifetime exceeding 100 μs. Although it is not clear why Pt-11 has such

a long luminescent lifetime at room temperature due to both low k_r and k_{nr} values, the distinction of Pt-11, Pt-12, and Pt-13 from the rest of Pt(N^C^N)Cl complexes suggests that the luminescent properties of the Pt(N^C^N)Cl complexes could be significantly modified by changing the nature of electron-accepting groups even though the structure of the core segment Pt−N−C−N is largely unaffected (Figure 2).

All of the Pt(N^C^N)X complexes have the structured luminescent spectra displaying resolved vibronic progressions. Two prominent vibronic features are presented in the emission spectra (Figure 5). The intensity ratio of the first major vibronic transition to the highest energy peak ($E_{em}(0-0)$) is a measure of vibronic coupling between the ground and excited states (Huang−Rhys factor, S_M) and is proportional to the degree of structural distortion that occurs in the excited state relative to the ground state.[49−52] The dominant vibrational mode associated with the excited state distortion ($\hbar\omega_M$) can be obtained from the energy difference (in cm^{-1}) of these vibronic transitions at 77 K, whereas the S_M value can be estimated from the peak heights. As illustrated in Figure 5, the values of the vibronic spacing for all of the selected Pt complexes are the same within experimental error ($\hbar\omega_M \approx 1300$ cm^{-1}). For three Pt complexes with the same core segment (i.e., Pt-1, Pt-4, and Pt-9), the Huang−Rhys factors also increase monotonically with decreasing $E_{em}(0-0)$, and the S_M value of Pt-9 is larger than those of Pt-1 and Pt-4.

Ground-State and Excited-State Properties of Pt-(N^C^N)X. The lowest energy excited state of square planar d^8 metal complexes has been studied intensely during the past two decades. However, it has been focused on how to raise the energy level of the metal-centered (d−d) excited state and how to prevent potential quenching of the luminescence of Pt complexes.[16,21−24] It lacks a systematic and detailed study to correlate the nature of the excited state of Pt complexes (e.g., ^{3}MLCT, ^{3}LC, and ^{1,3}ILCT) with their luminescent properties. Although it is well documented that the excited state of a Pt(N^C^N)X like Pt-1 has a majority of ^{3}LC characters mixed with some ^{1}MLCT/^{3}MLCT components,[15,18] it is still very valuable to explore why Pt-1 is more emissive than most of the literature reported Pt complexes.

The emission properties of Pt-1 have been compared with those of its analogs, i.e., ppyPt(acac),[16] platinum (2-phenyl-pyridinato-N,C2′) (pyridine) chloride [ppyPt(py)Cl],[53] and Pt(phbpy)Cl[23] (Scheme S1 shows the structure of these complexes), which have similar coordination spheres consisting of two pyridinyl rings, one cyclometalated phenyl ring, and one chloride. The absorption and room temperature emission spectra of these four complexes are shown in Figure 6, and their photophysical data are presented in
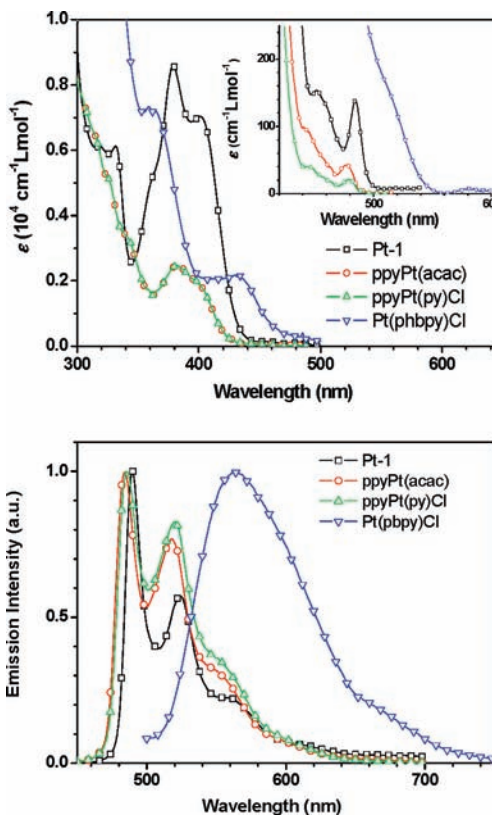

Figure 6. The comparison of absorption spectra (top) and emission spectra (bottom) of Pt-1, ppyPt(acac), ppyPt(py)Cl, and Pt(pbbpy)Cl in CH_2Cl_2 at room temperature. The T_1 absorption transitions are shown in the inset.

Table 7. Emission Properties of Pt-1 and Pt-12 and Their Analogs at Room Temperature

	λ_{max} (nm)	τ (μs)	Φ_{PL}	k_r (10^5 s^{-1})	k_{nr} (10^5 s^{-1})
Pt-1[17a]	490	7.2	0.60	0.83	0.55
ppyPt(acac)[16]	484	2.6	0.15	0.57	3.2
ppyPt(py)Cl	485	1.8	0.002	0.011	5.5
Pt(phbpy)Cl[41a]	563	0.5	0.025	0.5	19.5
Pt-12	592	3.5	0.072	0.21	2.7
piqPt(acac)	592	4	0.08	0.2	2.3

Table 7. The high quantum yield of Pt-1 can be attributed to its high radiative decay rate and low nonradiative decay rate. Although both ppyPt(acac) and ppyPt(py)Cl are similar to Pt-1 in terms of emission energies, structured emission spectra, and well-resolved triplet absorption spectra, they appeared to have higher MLCT transition energies than Pt-1 (Figure 6a), associated with higher reduction values. The potential larger energy difference between the MLCT state and ^{3}LC state could result in a weaker mixing of both singlet and triplet MLCT components into the excited state for ppyPt(acac) and ppyPt(py)Cl. This analysis is supported by the fact that Pt-1 has a higher k_r value, a higher extinction coefficient of triplet absorption, and less pronounced vibronic features of the emission spectrum (smaller Huang−Rhys factor; Figure 6 and Table 7).[54] A similar trend was observed for the comparison between red-emitting Pt-12 and its analog platinum(2-phenyl-isoquinolyl-N,C2′) acetylacetonate [piqPt(acac)],[55] although both complexes have

(47) Caspar, J. V.; Westmoreland, T. D.; Allen, G. H.; Bradley, P. G.; Meyer, T. J.; Woodruff, W. H. *J. Am. Chem. Soc.* **1984**, *106*, 3492.

(48) Damrauer, N. L.; Boussie, T. R.; Devenney, M.; McCusker, J. K. *J. Am. Chem. Soc.* **1997**, *119*, 8253.

(49) Caspar, J. V.; Westmoreland, T. D.; Allen, G. H.; Bradley, P. G.; Meyer, T. J.; Woodruff, W. H. *J. Am. Chem. Soc.* **1984**, *106*, 3492.

(50) Rillema, D. P.; Blanton, C. B.; Shaver, R. J.; Jackman, D. C.; Boldaji, M.; Bundy, S.; Worl, L. A.; Meyer, T. J. *Inorg. Chem.* **1992**, *31*, 1600.

(51) Allen, G. H.; White, R. P.; Rillema, D. P.; Meyer, T. J. *J. Am. Chem. Soc.* **1984**, *106*, 2613.

(52) Damrauer, N. L.; Boussie, T. R.; Devenney, M.; McCusker, J. K. *J. Am. Chem. Soc.* **1997**, *119*, 8253.

(53) Mdleleni, M. M.; Bridgewater, J. S.; Watts, R. J.; Ford, P. C. *Inorg. Chem.* **1995**, *34*, 2334.

(54) Li, J.; Djurovich, P. I.; Alleyne, B. D.; Yousufuddin, M.; Ho, N. N.; Thomas, J. C.; Peters, J. C.; Bau, R.; Thompson, M. E. *Inorg. Chem.* **2005**, *44*, 1713.
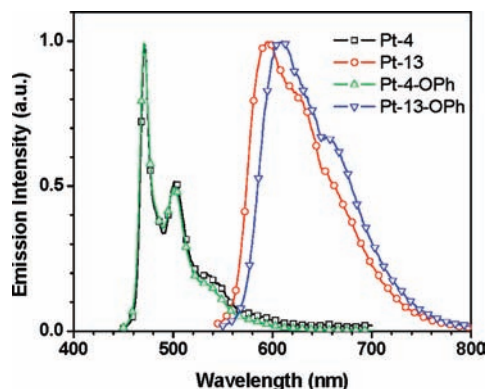
Figure 7. The comparison of emission spectra of Pt-4, Pt-4-OPh, Pt-13, and Pt-13-OPh in CH_2Cl_2 at room temperature.

lower quantum yields than their green-emitting analogs (Figure S1). Compared with Pt-1, Pt(phbpy)Cl has different excited state characteristics, i.e., [3]MLCT, which results in emission and absorption spectra with much fewer features.[23] The low quantum yield of Pt(phbpy)Cl can be attributed to a comparably low radiatve decay rate and a much faster non-radiative decay process due to possible d−d quenching.[17a,56]

The excited state properties of the Pt($N^\wedge C^\wedge N$)X complexes are strongly dependent on the chemical structures. The change of functional groups on the phenyl ring of Pt-1 will not only modify the emission energy but also the nature of the excited state. For example, adding electron donating groups to the phenyl rings (e.g., Pt-9) lowers the radiative decay rate and increases the Huang−Ryes factor, indicating a smaller component of [1]MLCT/[3]MLCT character in the lowest excited state. Replacing the pyridinyl group with isoquinonyl groups also leads to a 10-fold drop in the radiative decay rate, which results in a much lower quantum yield for Pt-12 and Pt-13 than most literature reported Pt($N^\wedge C^\wedge N$)Cl complexes.[17] The comparison of photophysical properties between Pt-12 and piqPt(acac) indicates that the nature of electron-accepting groups could strongly influence the excited state properties of both Pt($N^\wedge C^\wedge N$)Cl and Pt($C^\wedge N$)(acac) complexes (Figure S1).

Three Pt($N^\wedge C^\wedge N$)(OPh) complexes were examined using similar $N^\wedge C^\wedge N$-coordinating ligands (Table 6 and Figure 7). The change of ancillary ligands does not modify the oxidation or reduction potentials of corresponding Pt complexes significantly, and both Pt−Cl and Pt−OPh complexes have similar emission spectra. However, Pt−OPh complexes have around one-half the quantum yields of their Pt−Cl analogs due to comparably lower k_r values (for Pt-12-OPh and Pt-13-OPh) and higher k_{nr} values (for Pt-4-OPh). This indicates that the ancillary ligands can influence the excited state properties

of Pt($N^\wedge C^\wedge N$)X complexes through Pt−X interaction, even though the excited state localizes mainly in the Pt−N−C−N fragment.[15,17] The study of Pt($N^\wedge C^\wedge N$)(OPh) complexes provides an alternative route to developing halogen-free phosphorescent emitters which can be used to improve the operational stability of blue and white OLEDs.[17b,57]

Conclusion

Facile synthesis of platinum *m*-di(2-pyridinyl)benzene chloride and its derivatives, using controlled microwave heating, was reported. This method not only shortened the reaction time but also improved the reaction yield for most of the Pt complexes. Moreover, the reaction yield is dependent on the identity of substituents on the centered phenyl rings. A possible reaction mechanism for the metal coordination reaction was proposed as a multicentered pathway of nucleophile-assisted electrophilic reaction. Such a high-throughput synthetic method will help us build a database for this class of Pt complexes and enable us to explore their potential utilities in OLEDs and other applications thoroughly.

The electrochemical and photophysical properties of a series of Pt($N^\wedge C^\wedge N$)X complexes are discussed in detail. The electrochemical studies of all Pt complexes demonstrate that the oxidation process occurs on the metal-phenyl fragment and the reduction process is associated with the electron-accepting groups like pyridinyl groups and their derivatives. The lowest excited state of Pt($N^\wedge C^\wedge N$)X complexes is identified as a dominant ligand-centered [3]$\pi−\pi$* state with some MLCT character, which appears to have a larger [1]MLCT component than Pt($C^\wedge N$)(LX) and Pt($C^\wedge N^\wedge N$)Cl analogs. This results in a high radiative decay rate and high quantum yield for Pt(dpb)Cl and its analogs. However, the excited state properties of the Pt($N^\wedge C^\wedge N$)X complexes are strongly dependent on the nature of the electron-accepting groups and substituents to the metal-phenyl fragment. A rational design will be needed to tune the emission energies of the Pt($N^\wedge C^\wedge N$)X complexes over a wide range while maintaining their high luminescent efficiency. Most of the Pt-($N^\wedge C^\wedge N$)X complexes reported here are highly emissive and stable to sublimation, making them ideal as phosphorescent emitters for OLEDs. Devices fabricated with Pt-4 and Pt-8 have an external quantum efficiency of > 10% for monochromatic and white phosphorescent OLEDs.[7,17b]

(55) The structure and synthesis of platinum (2-phenyl-isoquinolyl-N, C2′) (acetylacetonate) [piqPt(acac)] is provided in the Supporting Information.

(56) Lai, S.-W.; Lam, H.-W.; Lu, W.; Cheung, K.-K.; Che, C.-M. *Organometallics* **2002**, *21*, 226−234.

(57) Giebink, N. C.; D'Andrade, B. W.; Weaver, M. S.; Mackenzie, P. B.; Brown, J. J.; Thompson, M. E.; Forrest, S. R. *J. Appl. Phys.* **2008**, *103*, 044509.